Chemical Engineering Journal 165 (2010) 714–719

Contents lists available at ScienceDirect

Chemical Engineering Journal

journal homepage: www.elsevier.com/locate/cej

Microworms self-assembled by boron nitride horns for optoelectronic applications

Zhi-Gang Chen [a], Lina Cheng [a], Gaoqing Lu [b], Jin Zou [a,c,*]

[a] Materials Engineering, University of Queensland, Brisbane, QLD 4072, Australia
[b] ARC Centre of Excellence for Functional Nanomaterials, University of Queensland, Brisbane, QLD 4072, Australia
[c] Centre for Microscopy and Microanalysis, University of Queensland, Brisbane, QLD 4072, Australia

ARTICLE INFO

Article history:
Received 22 March 2010
Received in revised form 26 July 2010
Accepted 31 July 2010

Keywords:
BN
Microworm
Horn
Light emission
Self-assembly

ABSTRACT

We report the self-assembly of microworms from boron nitride horns by chemical vapor deposition. Through advanced electron microscopy analysis of the intermediate products, the evolution of such microworms has been determined to be governed by a root-based growth mechanism, in which BN horns are initiated by the boron particles, self-intertwisted together to from worm-like structures, and finally formed into microworms. Strong light emissions are observed in such microworms, showing their high potential for applications in lasing, light-emitting diode, and medical diagnosis devices.

1. Introduction

Self-assembly, as an important synthesis method, has been extensively used to fabricate nanoscaled building blocks into complicated structures coupled with their superior electronic, magnetic or photonic properties for active optoelectronic devices and nano-electromechanical systems, such as integrated logic gates [1], field-effect transistors (FETs) [2,3], light-emitting diodes, laser diodes [4] and field emitters [5–7]. Many existing and emerging electronic/optoelectronic devices can greatly benefit from such complex integration into a single system in either two-dimensional (2D) or 3D layouts [8,9].

BN nanostructures with super thermal [10] and chemical stabilities [11–13] show great potential applications as unique electromechanical and optoelectronic components for laser, light-emitting diode, and medical diagnosis [9]. Various BN nanostructures, such as nanotubes (NTs) [14], nanobamboos [15], yard-glass BNNTs [16], nanowires [17], microbelts [18] and hollow nanoribbons [19], have been studied. Among them, a BN cone-shaped structure, called BN nanohorn, is of special interest since the deviations from a flat B-N hexagonal sheet surface are accompanied by the appearance of topological defects located at its apex. This type of nanostructures was often observed as a byproduct for the synthesized BNNTs and their yields were marginally low, except one case where a large-scale fabrication was achieved at very high temperature (1700 °C) and the synthesized products exhibited specific aggregation behavior [20]. For this reason, it still is a great challenge to search for more efficient methods to fabricate high purity BN horns. Especially, *in situ* self-assembly of such BN horns structures into integrated systems is in their early stage for practical applications.

In this study, we demonstrate self-assembly of high quality micro-sized worm-like structures composing of BN horns with large inner diameter and open tips via a chemical vapor deposition (CVD) method. Their morphology and structural characteristics were investigated by scanning electron microscopy (SEM) and transmission electron microscopy (TEM). Cathodoluminescence (CL) measurement is performed and strong light emission is observed at the room temperature, indicating their great potential applications in lasing, light-emitting diode, and medical diagnosis devices.

2. Experimental

BN architectures were synthesized at a temperature of 1240 °C by a floating catalyst method [16] in a multi-zone horizontal tube furnace. The central region of the furnace was heated to 1240 °C with a heating rate of 35 °C min^{-1} and maintained at this temperature for 60–100 min. High purity streams of Ar gas (at a rate of ~150 ml/min), H_2 gas (at a rate of ~20 ml/min) and NH_3 gas (at a rate of ~200 ml/min) were used as the carrier and reaction gases,

* Corresponding author at: Centre for Microscopy and Microanalysis, University of Queensland, Brisbane, QLD 4072, Australia.
E-mail address: j.zou@uq.edu.au (J. Zou).

1385-8947/$ – see front matter © 2010 Elsevier B.V. All rights reserved.
doi:10.1016/j.cej.2010.07.069

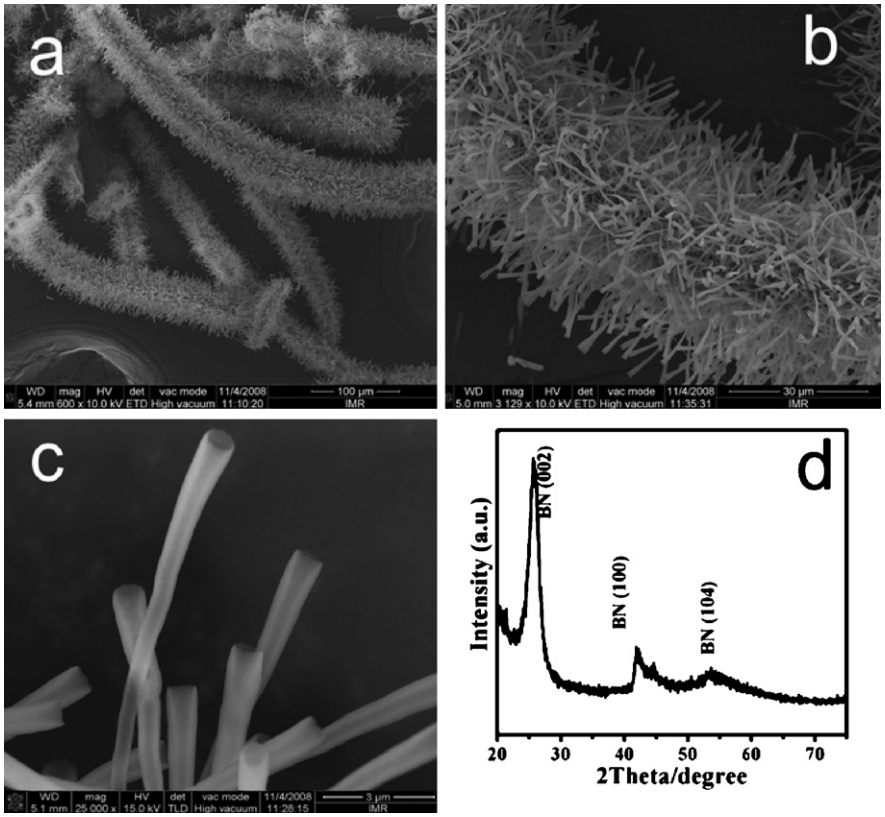

Fig. 1. (a) Low magnification SEM image showing several synthesized micro-sized architectures. (b) High magnification SEM image of a single BN architecture. (c) High magnification SEM image showing the cone-shape nanostructure. (d) XRD pattern of the synthesized architectures showing they are hexagonal BN structure.

respectively. The raw materials, ball milled mixture of B–O–Fe precursors with ratios of $B:B_2O_3:Fe_2O_3 = 1:7:2$, were loaded into a BN crucible at the center of an Al_2O_3 tube (diameter of 32 cm, length of 100 cm) which was located at the center of the furnace. After the furnace was cooled to room temperature naturally, white filament-like products were collected around the thermal couple above the crucible. Around 20 mg synthesized products can be collected for each synthesis, suggesting a yield of ~15% when compared with the B–O–Fe precursors used for the synthesis.

The synthesized products were characterized using X-ray diffraction (XRD, RINT2200, Cu Kα), scanning electron microscopy (SEM, LEO Super35) and transmission electron microscopy [TEM, Philips Tecnai F20 equipped with electron energy loss spectroscopy (EELS) and energy dispersive spectroscopy (EDS)]. Spatially resolved CL measurements and *in situ* CL imaging of BN architectures were carried out (TFE-SEM, Hitachi S4200). The synthesized BN architectures were spread on Si substrates for SEM and CL characterizations. CL spectra were collected using a high-resolution CL system operating at an accelerating voltage of 5 kV and a current of 1.2 nA. The specific surface area was determined from nitrogen adsorption-desorption isotherm at 77 K (ASAP 2010). The specific surface area of the synthesized BN architectures was estimated to be ~50 m^2/g.

3. Results and discussion

Fig. 1a–c are SEM images of synthesized architectures and show their general morphology. As shown in Fig. 1a, the synthesized products have worm-like morphology with their lateral dimension of several tens μm and their axial dimension of hundreds μm. Fig. 1b shows a magnified SEM image taken from a section of worm-like architecture; from which the architecture self-assembled by numerous tube-like structures can be seen. Fig. 1c is a high-magnification SEM image and shows detailed morphology of tube-like structures that form the worm-like architecture. As can be clearly seen, these nano-sized tubes are not parallel, rather resembling horns with typical cone-shaped morphology with open ends. Moreover, the open ends are relatively large with a diameter of several hundred nm. The comparison of Fig. 1b and Fig. 1c indicates that these horns grew randomly along the body of microworms. To understand the crystal structure(s) of synthesized projects, XRD analysis was carried out and Fig. 1d shows a typical XRD pattern taken from the synthesized products. By carefully analyzing the diffraction pattern, it is found that all diffraction peaks can be indexed by a hexagonal BN structure with the lattice parameters of $a = 0.250$ nm and $c = 0.665$ nm (JCPDS card: 45-0896). No other diffraction peaks were observed, suggesting that the synthesized products have a high purity of BN without impurities, such as B_2O_3 or other crystalline phases.

To understand the detailed structural characteristics of synthesized microworms, TEM was employed. Fig. 2a is a bright-field TEM image taken from a section of a typical microworm, similar to the SEM images. Fig. 2b is an enlarged TEM image taken near the truck of the microworm and displays their aggregation behaviors of horns. Such behaviors illustrate the small end tips intertwist each other and then form an aggregated morphology–microworm. Fig. 2c is a high-magnification TEM image, showing the open ends of typical horns. Fig. 2d is an entire horns peeling from the miroworms which show clear hollow morphology. The lateral diameters of these open ends vary from several hundred nm to μm. Based on our TEM investigation, the wall of horns can be estimated to be ~100 nm, which is much thicker than the reported nanohorns [20,21], which could be attributed to the synthesis low temperature.

The inset of Fig. 2d is a selected area electron diffraction (SAED) pattern obtained from a small area around the wall of a horn. Clearly

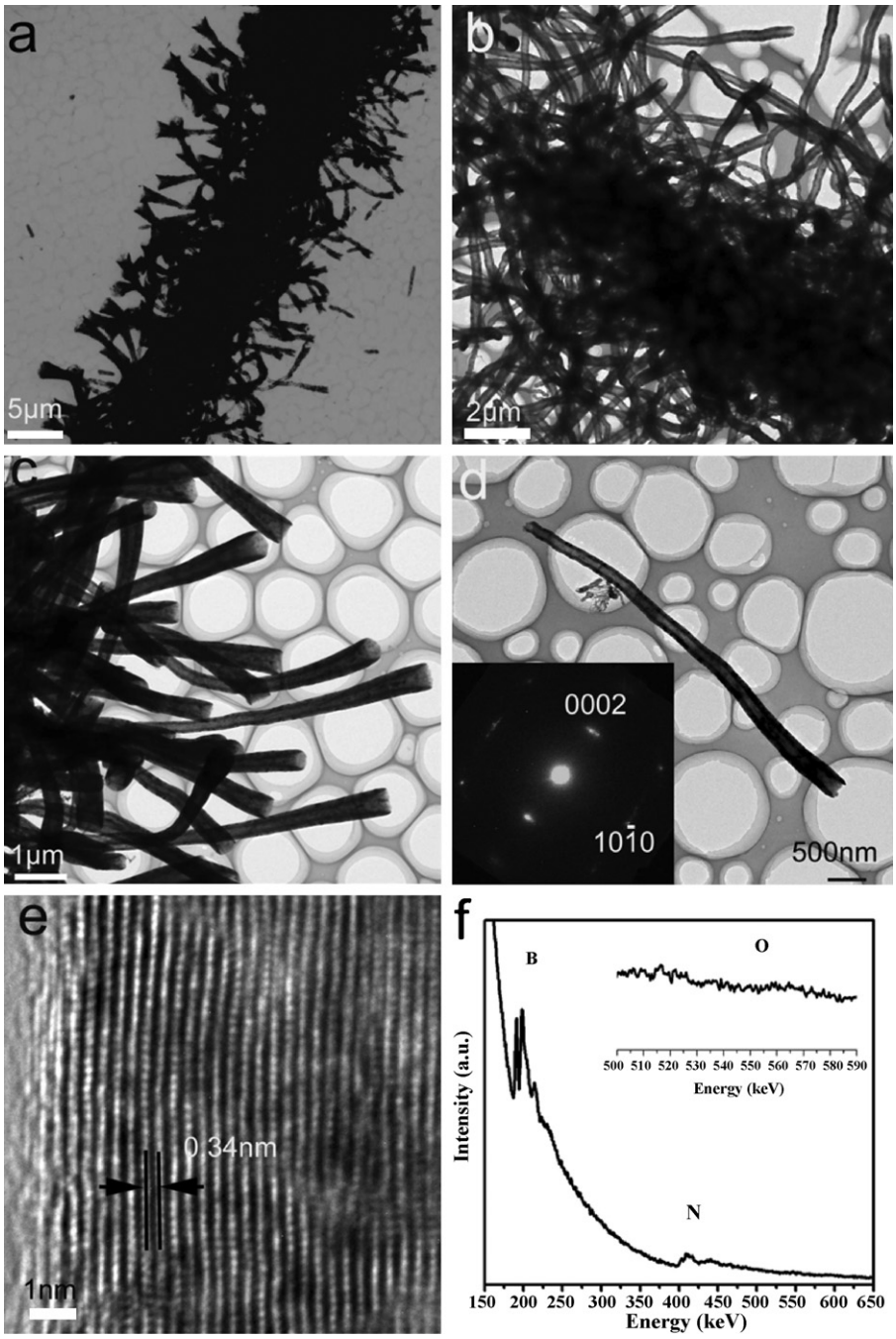

Fig. 2. (a) Low magnification TEM image of BN architecture assembled by numerous nanohorns. (b) Low magnification TEM image of a truck region. (c) High magnification TEM image showing cone-shape BN nanostructure. (d) A typical BN horn peeling from the architecture and inset being a SAED pattern showing $\{0\,0\,0\,2\}^*$ diffraction of the BN horn. (e) High resolution TEM image around the wall of a horn showing the wall is formed by basal BN sheets. (f) EELS analysis of a typical horn showing its high purity without contamination by other elements.

two diffraction spots perpendicular to the axial direction of the horn are seen. In fact, these two diffraction spots can be indexed as $(0\,0\,0\,2)^*$ diffraction spots for the hexagonal BN structure, indicating that the wall of the horn is formed by the wrapping of basal sheets of hexagonal BN structure. Fig. 2e is a high resolution TEM image taken from a section of the wall shown in Fig. 2c and shows that the wall is consisted of atomic planes with the lattice spacing of ~0.34 nm (corresponding to the $\{0\,0\,0\,2\}$ lattice spacing of hexagonal BN structure). To understand whether the synthesized BN microworms have contaminated by impurities, such as carbon or oxygen, EELS analysis was carried out on a number of BN microworms or individual horns. Fig. 2f shows a typical EELS profile and no carbon and oxygen were detected in the EELS profile (as shown in the inset of oxygen EELS profile), suggesting that the BN microworms or horns are pure hexagonal BN without contamination. In addition, sharp π^*-peaks can be seen on the left sides of both B and N K-edges, indicating that the tubes has the sp^2-bonding, i.e. the hexagonal structure. Quantitative analysis of all EELS spectra gives a B/N atomic ratio of 1.0 ± 0.1.

For understanding the growth mechanism of synthesized horns and their assembled microworms, we have carefully analyzed intermediate products, produced by reducing the reaction duration. Fig. 3a and b are SEM images of the products synthesized for less than 10 min. As can be seen, a large number of tadpole-shaped

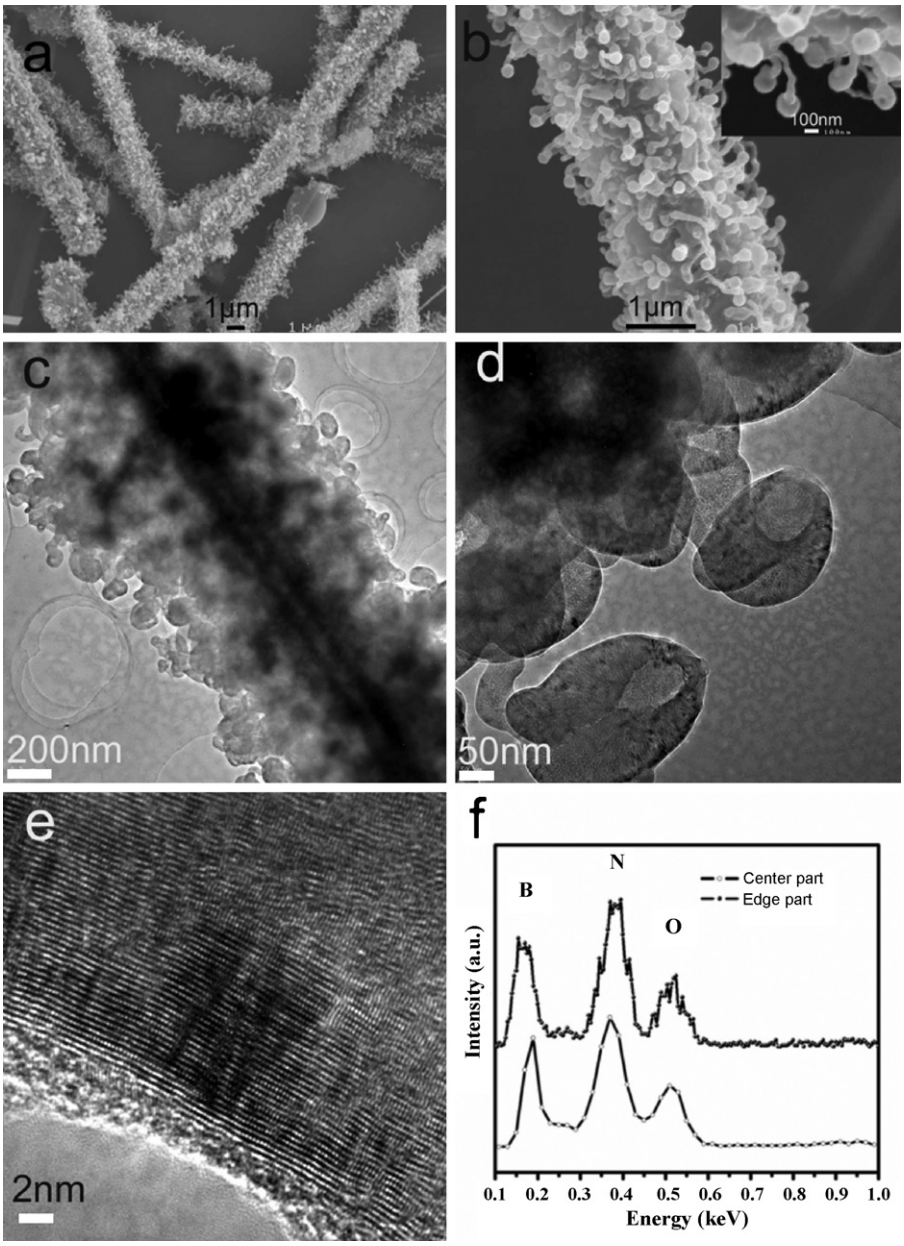

Fig. 3. (a) and (b) SEM images of intermediate products showing of the early formed architectures. (c) and (d) TEM images of the BN architectures showing open ends of flower-like BN structures. (e) HRTEM image of an open end showing the morphology. (f) EDS analyses of intermediate product confirming that the truck contains more B.

nanoparticles are self-assembled into a worm-like structure. It should be noted that the lateral dimension of the worm-like structure is in the order of 1 μm, distinctly smaller than that of obtained microworms [refer to Fig. 1a]. We anticipate that this should be the infantile structure of the microworms. From the corresponding TEM observations [refer to Fig. 3c and d], open ends can be seen in the form of flowers in bud at the heads of tadpoles, which further demonstrated the initial stage of the horns. Fig. 3e is a high resolution TEM image taken from the open ends and shows their typical lattice structures with the lattice spacing of ~0.34 nm (the distance of the basal planes of hexagonal BN structure). This indicates the open ends of the tadpoles have the hexagonal BN structure which similar to the BNNHs. To understand their chemical composition, EDS analysis was carried out. Fig. 3f is EDS spectra taken from the trunk and edge of the intermediate worm-like structures. From which, boron, nitrogen, and oxygen can be observed in both cases. Through quantitative analysis of EDS spectra, trunk regions contain more boron than the edge regions, indicating that trunk regions may be originally aggregated by the boron particles. That's, the infancy BN horns may be initiated by the boron particles which self-intertwisted together to from worm-like structures and finally to form mircoworms. This strongly suggests our BN horns governed by a root-based growth mechanism [22,23]. In our case, two reactions should govern the entire process and they are:

$$B + B_2O_3 \rightarrow BO, \quad (1)$$

$$BO + NH_3 \rightarrow BN + H_2O. \quad (2)$$

At the high temperature of 1240 °C, amorphous B powders react with B_2O_3 to form the intermediate products (BO) under the help of Fe_2O_3 catalysts in the B–O–Fe precursor. The intermediate products (BO) are easy to vaporize and react with ammonia to form boron and nitrogen atoms. The incoming boron and nitrogen atoms are incorporated into the BN honeycomb network (the BN honey-

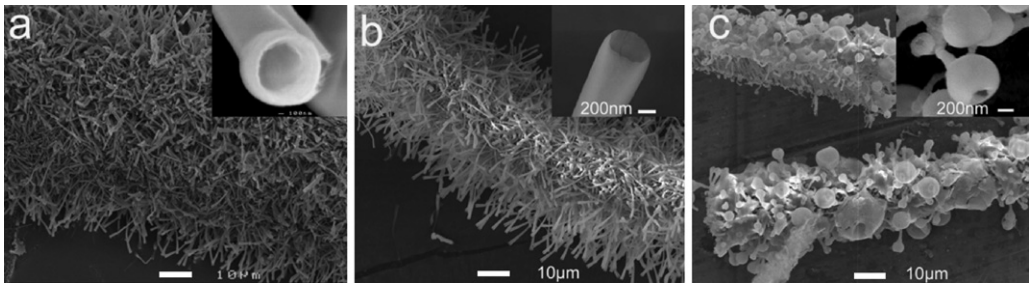

Fig. 4. SEM images of BN architectures synthesized at the temperature of 1200 (a), 1240 (b), and 1280 °C (c).

comb bonds are most reactive owing to the presence of defects [22]) at the bottom or the "root" of the forming BN horns. During the vaporizing reactions, the B–O–Fe precursor (the particle sizes of the B–O–Fe precursors are about several micrometers aggregated by nanoparticles with tens of nanometers, estimated by our SEM and TEM characterizations) is believed to decompose into elemental boron and nitrogen ions, which later agglomerate to form boron particles and later BNMWs. Such processing is relative long and has sufficient boron and nitrogen atoms to grow into thick and long BN horns. On a previous report [20], thin BN nanohorns were fabricated in super high temperature of 1700 °C using MgO as a catalyst. The growth of thin BN horns was hampered soon after the synthesis started, because Mg was oxidized to a solid MgO (the melting point of MgO is approximately 2800 °C, while the temperature in the growth area is less than 1700 °C) and then loses its catalytic activity. Therefore, this processing time would be much shorter and could result in the short lengths of thin BN horns [20].

To further understand the effect of the synthesis temperature on the morphology of fabricated BN architectures, the synthesis temperatures were varied (mainly 1200, 1240, 1280 °C) and the typical SEM images of the synthesis products are shown in Fig. 4. From which, the significant effect of the synthesis temperatures on the morphologies of BN architectures can be evidenced. With increasing the synthesis temperature, the BN horns tend to be large and their quality become poor, particular when the synthesis temperature reaches to 1280 °C. We also examined the effect of the concentration of NH_3 flow (varying the flow rates in the range of 100–250 ml/min) and found that the concentration of NH_3 has a little effect on the morphologies of BN architectures.

As mentioned above, one of the key applications of BN nanostructures and their architectures is in the field of optoelectronics. For this reason, the CL properties of the synthesized microworms were measured. Fig. 5a is a SEM image of a section of a microworm and Fig. 5b is its corresponding room temperature SEM-CL image taken with a wavelength of 341 nm. A uniform contrast can be

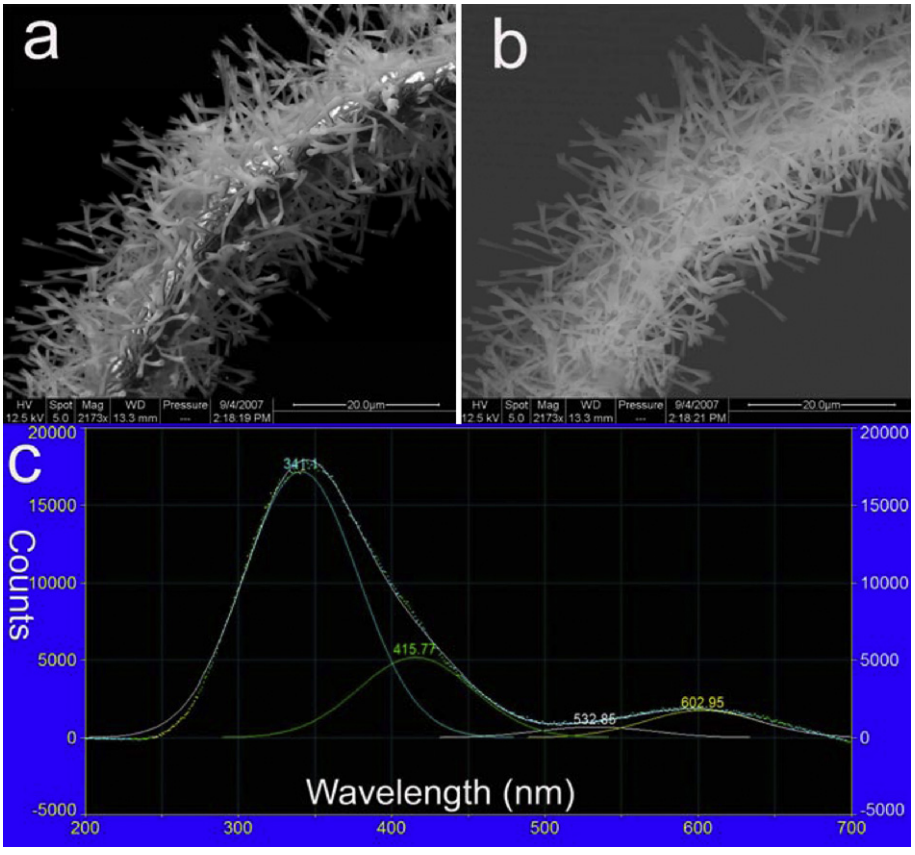

Fig. 5. (a) SEM image of a section of BN microworm. (b) SEM-CL image using the CL wavelength at 341 nm showing the uniform contrast across the BN microworm. (c) CL spectrum taken at room temperature.

observed in the SEM-CL image when compared its contrast and the microworm morphologies shown in both Fig. 5(a) and (b), indicating a uniform CL property across the entire microworm. Fig. 5c is a CL spectrum taken from the microworm at room temperature, similar to those reported in the literature [24–26]. There is a strong peak in the range of 200–500 nm and this peak exhibits asymmetric profile with a right-shoulder. In fact, this peak can be deconvoluted into two peaks, respectively centered at 341.1 and 415.77 nm, as shown in Fig. 4c. The peak centered at 341.1 nm (3.64 eV) is a typical CL emission from hexagonal BN structure or multi-walled cylindrical BNNTs [25,27], excited by high-energy electrons. This ultraviolet light emission was very stable after the sample was irradiated for 10 min. The peak (centered at 415.77 nm, corresponding 2.98 eV) is most likely associated with the large diameter conical structured BN nanostructures as the emission at the same energy range was only observed from BNNHs [20], suggesting that they are attributed to deep-level emissions associated with defect-related centers (B or N vacancy-type defect-trapped states). The spectrum has two additional band emissions centered at around 532.85 (2.33 eV) and 602.95 nm (2.57 eV), respectively. These visible band emissions may be attributed to large curve in the assembly processing. In fact, visible emissions at 490 nm from Eu-doped bamboo BNNTs [28] and ~550 nm from Si-doped bamboo BNNTs [29] have already been reported. The electronic structure of BNNHs has been theoretically studied [30,31]. The band-gap of B31N31 nanohorn was found to be 0.8 eV by the molecular orbital calculation [30], while a more reasonable band-gap at ~3.0 eV was determined by the density function theory calculation [31]. Therefore, the variable CL peak positions (ultraviolet and visible emissions) for BNMWs could be induced by intrinsic structural characteristics cased by impurities, defects, or B and N vacancies in individual BNNHs. Apparently, these ultraviolet and visible emissions are very useful for the optoelectronic applications in scatheless biological essay and medial analysis. Our study also indicates that the light emission from near-UV to near-red light range can be tuned by structural engineering (such as introducing defects through self-assembly).

4. Conclusions

In this study, BN microworms self-assembled from boron nitride horns were fabricated by a facile chemical vapor deposition method. The BN horns with a conical hollow structure and tens of μm in length are self-assembled to form microworms with tens of μm in diameter and hundreds of micrometers in length. From detailed characterizations of intermediate products, the infancy BN horns are initiated by the boron particles, then self-intertwisted together to from worm-like structures and finally to form mircoworms. Such growth is governed by a root-based growth mechanism. Strong light emissions at ultraviolet and visible regions are observed in such microworms, indicating their potential applications in lasing, light-emitting diode, and medical diagnosis devices.

Acknowledgment

we acknowledge the Australian Research Council, and the UQ start-up and UQ ECR grants for their financial supports to this study. We also thank Prof. H.-M. Cheng for kind help and discussion.

References

[1] A. Bachtold, P. Hadley, T. Nakanishi, C. Dekker, Logic circuits with carbon nanotube transistors, Science 294 (2001) 1317–1320.
[2] X.F. Duan, Y. Huang, Y. Cui, J.F. Wang, C.M. Lieber, Indium phosphide nanowires as building blocks for nanoscale electronic and optoelectronic devices, Nature 409 (2001) 66–69.
[3] Y.M. Lin, J. Appenzeller, Z.H. Chen, Z.G. Chen, H.M. Cheng, P. Avouris, High-performance dual-gate carbon nanotube FETs with 40-nm gate length, IEEE Electron Device Lett. 26 (2005) 823–825.
[4] M. Zhang, S.L. Fang, A.A. Zakhidov, S.B. Lee, A.E. Aliev, C.D. Williams, K.R. Atkinson, R.H. Baughman, Strong, transparent, multifunctional, carbon nanotube sheets, Science 309 (2005) 1215–1219.
[5] Z.G. Chen, L.N. Cheng, H.Y. Xu, J.Z. Liu, J. Zou, T. Sekiguchi, G.Q. Lu, H.M. Cheng, ZnS branched architectures as optoelectronic devices and field emitters, Adv. Mater. 22 (2010) 2376–2380.
[6] Z.G. Chen, J. Zou, G. Liu, X.D. Yao, F. Li, X.L. Yuan, T. Sekiguchi, G.Q. Lu, H.M. Cheng, Growth, cathodoluminescence and field emission of ZnS tetrapod tree-like heterostructures, Adv. Funct. Mater. 18 (2008) 3063–3069.
[7] Z.G. Chen, J. Zou, D.W. Wang, L.C. Yin, G. Liu, Q.F. Liu, C.H. Sun, X.D. Yao, F. Li, X.L. Yuan, T. Sekiguchi, G.Q. Lu, H.M. Cheng, Field emission and cathodoluminescence of ZnS hexagonal pyramids of zinc blende structured single crystals, Adv. Funct. Mater. 19 (2009) 484–490.
[8] J.H. Ahn, H.S. Kim, K.J. Lee, S. Jeon, S.J. Kang, Y.G. Sun, R.G. Nuzzo, J.A. Rogers, Heterogeneous three-dimensional electronics by use of printed semiconductor nanomaterials, Science 314 (2006) 1754–1757.
[9] J.C.S. Wu, S.J. Lin, Novel BN supported bi-metal catalyst for oxydehydrogenation of propane, Chem. Eng. J. 140 (2008) 391–397.
[10] W.Q. Han, W. Mickelson, J. Cumings, A. Zettl, Transformation of BxCyNz nanotubes to pure BN nanotubes, Appl. Phys. Lett. 81 (2002) 1110–1112.
[11] D. Golberg, Y. Bando, C.C. Tang, C.Y. Zhi, Boron nitride nanotubes, Adv. Mater. 19 (2007) 2413–2432.
[12] Y. Chen, J. Zou, S.J. Campbell, G. Le Caer, Boron nitride nanotubes: pronounced resistance to oxidation, Appl. Phys. Lett. 84 (2004) 2430–2432.
[13] Z.G. Chen, J. Zou, G.Q. Lu, G. Liu, F. Li, H.M. Cheng, ZnS nanowires and their coaxial lateral nanowire heterostructures with BN, Appl. Phys. Lett. 90 (2007) 103117.
[14] N.G. Chopra, R.J. Luyken, K. Cherrey, V.H. Crespi, M.L. Cohen, S.G. Louie, A. Zettl, Boron-nitride nanotubes, Science 269 (1995) 966–967.
[15] R.Z. Ma, Y. Bando, T. Sato, Controlled synthesis of BN nanotubes, nanobamboos, and nanocables, Adv. Mater. 14 (2002) 366–368.
[16] Z.G. Chen, J. Zou, F. Li, G. Liu, D.M. Tang, D. Li, C. Liu, X.L. Ma, H.M. Cheng, G.Q. Lu, Z.D. Zhang, Growth of magnetic yard-glass shaped boron nitride nanotubes with periodic iron nanoparticles, Adv. Funct. Mater. 17 (2007) 3371–3376.
[17] K.F. Huo, Z. Hu, F. Chen, J.J. Fu, Y. Chen, B.H. Liu, J. Ding, Z.L. Dong, T. White, Synthesis of boron nitride nanowires, Appl. Phys. Lett. 80 (2002) 3611–3613.
[18] Z.G. Chen, J. Zou, Q.L. Liu, C.H. Sun, G. Liu, X.D. Yao, F. Li, B. Wu, X.L. Yuan, T. Sekiguchi, H.M. Cheng, G.Q. Lu, Self-assembly and cathodoluminescence of microbelts from Cu-doped boron nitride nanotubes, ACS Nano 2 (2008) 1523–1532.
[19] Z.G. Chen, J. Zou, G. Liu, F. Li, Y. Wang, L.Z. Wang, X.L. Yuan, T. Sekiguchi, H.M. Cheng, G.Q. Lu, Novel boron nitride hollow nanoribbons, ACS Nano 2 (2008) 2183–2191.
[20] C.Y. Zhi, Y. Bando, C.C. Tang, D. Golberg, R.G. Xie, T. Sekiguchi, Large-scale fabrication of boron nitride nanohorn, Appl. Phys. Lett. 87 (2005) 63107–63109.
[21] T. Oku, K. Hiraga, T. Matsuda, Growth of boron nitride nanohorn structures, Mater. Trans. 49 (2008) 2461–2464.
[22] R.S. Lee, J. Gavillet, M.L. de la Chapelle, A. Loiseau, J.L. Cochon, D. Pigache, J. Thibault, F. Willaime, Catalyst-free synthesis of boron nitride single-wall nanotubes with a preferred zig-zag configuration, Phys. Rev. B 64 (2001), 121405-121401–121405-121404.
[23] X. Blase, A. De Vita, J.C. Charlier, R. Car, Frustration effects and microscopic growth mechanisms for BN nanotubes, Phys. Rev. Lett. 80 (1998) 1666–1669.
[24] T. Sekiguchi, S. Koizumi, T. Taniguchi, Characterization of P–N junctions of diamond and c-BN by cathodoluminescence and electron-beam-induced current, J. Phys. Condens. Matter 16 (2004) S91–S97.
[25] C.Y. Zhi, Y. Bando, C.C. Tang, R.G. Xie, T. Sekiguchi, D. Golberg, Perfectly dissolved boron nitride nanotubes due to polymer wrapping, J. Am. Chem. Soc. 127 (2005) 15996–15997.
[26] Z.G. Chen, J. Zou, G. Liu, F. Li, H.M. Cheng, T. Sekiguchi, M. Gu, X.D. Yao, L.Z. Wang, G.Q. Lu, Long wavelength emissions of periodic yard-glass shaped boron nitride nanotubes, Appl. Phys. Lett. 94 (2009) 023105.
[27] J.S. Lauret, R. Arenal, F. Ducastelle, A. Loiseau, M. Cau, B. Attal-Tretout, E. Rosencher, L. Goux-Capes, Optical transitions in single-wall boron nitride nanotubes, Phys. Rev. Lett. 94 (2005) 037405–037407.
[28] H. Chen, Y. Chen, C.P. Li, H.Z. Zhang, J.S. Williams, Y. Liu, Z.W. Liu, S.P. Ringer, Eu-doped boron nitride nanotubes as a nanometer-sized visible-light source, Adv. Mater. 19 (2007) 1845–1848.
[29] S.F. Xu, Y. Fan, J.S. Luo, L.G. Zhang, W.Q. Wang, B. Yao, L.N. An, Phonon characteristics and photoluminescence of bamboo structured silicon-doped boron nitride multiwall nanotubes, Appl. Phys. Lett. 90 (2007) 13115–13117.
[30] A. Nishiwaki, T. Oku, I. Narita, Formation and atomic structures of boron nitride nanohoms, Sci. Tech. Adv. Mater. 5 (2004) 629–634.
[31] M. Machado, P. Piquini, R. Mota, Electronic properties of selected BN nanocones, Mater. Charact. 50 (2003) 179–182.